Infection and Immunity

Pasteurella multocida Toxin as a Transporter of Non-Cell-Permeating Proteins

Stefan Bergmann, Doris Jehle, Carsten Schwan, Joachim H. C. Orth and Klaus Aktories

---

Updated information and services can be found at:
http://iai.asm.org/content/81/7/2459

These include:

SUPPLEMENTAL MATERIAL   Supplemental material

REFERENCES   This article cites 50 articles, 22 of which can be accessed free
at: http://iai.asm.org/content/81/7/2459#ref-list-1

CONTENT ALERTS   Receive: RSS Feeds, eTOCs, free email alerts (when new
articles cite this article), more»

Information about commercial reprint orders: http://journals.asm.org/site/misc/reprints.xhtml
To subscribe to to another ASM Journal go to: http://journals.asm.org/site/subscriptions/

Journals.ASM.org

Pasteurella multocida Toxin as a Transporter of Non-Cell-Permeating Proteins

Stefan Bergmann,[a] Doris Jehle,[a] Carsten Schwan,[a] Joachim H. C. Orth,[a] Klaus Aktories[a,b]

Institut für Experimentelle und Klinische Pharmakologie und Toxikologie, Albert-Ludwigs-Universität Freiburg, Freiburg, Germany[a]; BIOSS Centre for Biological Signalling Studies, Universität Freiburg, Freiburg, Germany[b]

The protein toxin *Pasteurella multocida* toxin (PMT) is the causative agent of atrophic rhinitis in pigs, leading to atrophy of the nasal turbinate bones by affecting osteoblasts and osteoclasts. The mechanism of PMT-induced intoxication is a deamidation of α-subunits of heterotrimeric G proteins, including $G\alpha_q$, $G\alpha_{13}$, and $G\alpha_i$, thereby causing persistent activation of the G proteins. Here we utilized PMT as a transporter of the non-cell-permeating A domain of diphtheria toxin (DTa). Fusion proteins of PMT and DTa ADP-ribosylated elongation factor 2, the natural target of diphtheria toxin, leading to cell toxicity. PMT-DTa effects were competed by PMT, indicating binding to the same cell surface receptor. Fluorescently labeled PMT-DTa and PMT colocalized with specific markers of early and late endosomes. Bafilomycin A, which inhibits vacuolar H^+-ATPase, blocked PMT-DTa-induced intoxication of HEK-293 cells. By constructing various PMT-DTa chimeras, we identified a minimal region of PMT necessary for uptake of DTa. The data suggest that PMT is able to transport cargo proteins into eukaryotic cells by utilizing the PMT-specific uptake route.

*P*asteurella multocida is a frequent commensal of the respiratory tract of animals. As a facultative pathogen, it can lead to severe and economically important diseases, such as shipping fever in cattle, snuffles in rabbits, and fowl cholera in poultry (1). Zoonotic diseases normally arise from scratches, bites, and saliva from pet animals such as cats and dogs (2, 3). One of the major virulence factors of *P. multocida* is the protein toxin PMT (*P. multocida* toxin), which is produced by serogroup D and some A strains (4). PMT is the causative agent to induce atrophic rhinitis in pigs. This disease is characterized by shortening and twisting of the snout due to the loss of nasal turbinate bones (5, 6).

PMT activates various heterotrimeric G proteins (7, 8). Recently, we identified the molecular mechanism of the toxin as a deamidation of the α-subunits of heterotrimeric G proteins (9). An essential glutamine residue in the switch II region of the GTPase domain of α-subunits is deamidated, resulting in a glutamic acid. Because the targeted glutamine is crucial for GTP hydrolysis by G proteins (10), PMT-deamidated G proteins are constitutively activated. Many heterotrimeric G proteins are substrates of the toxin. PMT activates the $G\alpha_{q/11}$ family to induce phospholipase Cβ stimulation and, subsequently, stimulates Ca^{2+} and protein kinase C signaling (11, 12). Also, $G\alpha_{12/13}$ proteins, which trigger RhoA activation via RhoGEF proteins, are targets of the toxin (13, 14). Moreover, PMT activates $G\alpha_{i1-3}$, leading to inhibition of the adenylyl cyclase (15). However, the fourth family of heterotrimeric G proteins, $G\alpha_s$, is not a substrate of PMT. Besides activating α-subunits of G proteins, the toxin induces the release of Gβγ, thereby stimulating Gβγ-dependent signaling. For example, phosphoinositide-3-kinase γ is stimulated by this signaling pathway (16). PMT-induced activation of G proteins leads to strong mitogenic and antiapoptotic effects and affects cell differentiation processes (17–19). Notably, the identical glutamine residue of $G\alpha_{q/11}$, which is targeted by PMT, was identified as a mutation site in melanoma and blue nevi (20).

The 146-kDa toxin PMT is a one-chain toxin comprising 1,285 amino acids (aa) (7). Different domains of PMT are involved in cell uptake and intracellular action. The receptor binding and translocation domains are located in the N terminus (aa 1 to 574). Whereas the receptor binding domain has not been characterized in detail, two amphipathic helices, covering residues 402 to 457, are suggested to be involved in membrane insertion and translocation (21). So far, the cell surface receptor of PMT is not known (22). The biologically active C-terminal part of PMT (aa 575 to 1285) was crystallized, and the structure revealed 3 domains (23). Domain C1 (aa 575 to 719) has homology to the N-terminal portion of clostridial glycosyltransferases. It functions as an intracellular membrane localization domain (24, 25). Whereas no function has been assigned to domain C2 (aa 720 to 1104), the C3 domain (aa 1105 to 1285) harbors the catalytic deamidase activity of PMT. This domain exhibits homology to papain-like cysteine proteases. The catalytic triad consists of Cys-1165, His-1205, and Asp-1220 (23, 26–28).

Diphtheria toxin (DT) consists of three domains. The catalytically active domain (DTa) is localized at the N terminus, followed by the translocation (T) domain and the receptor binding (R) domain in the C terminus (29, 30). During uptake, the active part (DTa) has to be cleaved by host proteases. Additionally, a disulfide bond between the proteolytically cleaved DTa and the translocation domain has to be reduced to release fully active DTa into the cytosol (31). In the cytosol, DTa transfers an ADP-ribose moiety from NAD^+ onto elongation factor 2 (EF-2) (32, 33). The accep-

tor amino acid is diphthamide, a posttranslationally modified histidine residue. ADP-ribosylation of EF-2 by DTa inhibits protein synthesis and results in death of target cells (34).

Here we present the construction of PMT-DTa fusion proteins on the basis of a non-cell-permeating DT fragment (DTa) and distinct fragments of PMT. The obtained fusion proteins reveal regions of PMT that transport a cargo protein into the cytosol of host cells. Additionally, fusion proteins were characterized in respect to specific steps of their uptake into host cells, e.g., receptor binding, intracellular trafficking, or pH-dependent translocation from endosomes into the cytosol.

MATERIALS AND METHODS

Materials. PCR primers were from Apara (Denzlingen, Germany). Diphtheria toxin was purchased from Calbiochem, and ^{32}P-NAD$^+$ and [^{14}C]leucine were purchased from PerkinElmer (Cologne, Germany). All other reagents were of analytical grade and were purchased from commercial sources.

Cloning and expression of PMT-DTa chimeras. The plasmid encoding the PMT-DTa chimera was generated by using the PMT^{C1165S}-pGEX2T construct (26). DTa (aa 26 to 216) was amplified with the following primer pair harboring BamHI restriction sites: DTa^{26}sense (5'-ATAGGATCCGGC GCTGATGATGTTGTTGATTCTTC-3') and DTa^{216}anti (5'-ATAGGAT CCGACACGATTTCCTGCACAGGCTTGAG-3'). PMT^{C1165S}-pGEX2T was digested at the 3' end with BamHI, and the DTa fragment was ligated into the open vector. The plasmids encoding PMT$^{\Delta C}$-DTa, PMT^{505}-DTa, and PMT^{400}-DTa were generated by standard PCR techniques utilizing the PMT-DTa-pGEX2T construct and the primer DTa^{26}sense (5'-GCAC TAGGATCCGGCGCTGATGATGTTGTTGAT-3'). The following corresponding primers were used: for PMT$^{\Delta C}$-DTa (PMT aa 1 to 582), PMT^{582}anti (5'-AGGACTATAAGGAGAGCCCCCTAATAGTTTAG-3'); for PMT^{505}-DTa (PMT aa 1 to 505), PMT^{505}anti (5'-AGGAGGATC ATCAGGTGAGATAGAATGTAA-3'); and for PMT^{400}-DTa (PMT aa 1 to 400), PMT^{400}anti (5'-TATTGCAGATAACTGTGAAATAAAGGTTT C-3').

PMT, the catalytically inactive mutant PMT^{C1165S}, and all PMT-DTa fusion proteins were expressed and purified as described previously (26).

Cell culture. HEK-293 cells were cultured in Dulbecco's modified Eagle's medium (DMEM) supplemented with 10% fetal calf serum (FCS) and 1% penicillin-streptomycin (P/S) in an atmosphere of 5% CO$_2$ at 37°C. The Caco-2 cell line was cultured in DMEM supplemented with 10% FCS, 1% P/S, 1% nonessential amino acids, and 1% sodium pyruvate. Cell lysates were prepared as follows. HEK-293 cells were washed twice with phosphate-buffered saline (PBS) (4°C), lysed in RIPA buffer (50 mM HEPES, 150 mM NaCl, 1% Triton X-100, 0.5% sodium desoxycholate, and 0.1% SDS) at 4°C, and centrifuged for 20 min at 14,000 rpm. Supernatants were used as cell lysates.

Trypsin activation. Diphtheria toxin (6.3 μM) dissolved in PBS was incubated with 0.75 ng trypsin for 30 min at 25°C, and then 0.1 M dithiothreitol (DTT) was added for another 15 min (37°C). For activation of the PMT-DTa chimeras, equimolar amounts of fusion proteins were treated as mentioned above.

ADP-ribosylation of EF-2. Twenty-five micrograms of HEK-293 cell lysate was incubated for 30 min at 37°C with 4.6 kBq radioactive ^{32}P-NAD$^+$ and toxin chimera at the indicated concentrations in 20 μl ADP-ribosylation buffer (1 mM EDTA, 50 mM NaCl, 50 mM Tris-HCl [pH 7.5], 1 mM DTT, and 5 mM thymidine). Radiolabeled proteins were detected by SDS-PAGE and subsequent phosphorimaging (Molecular Dynamics). For post-ADP-ribosylation, HEK-293 cells were incubated with PMT-DTa (3 nM) for 6 h. After changing of the medium and further incubation overnight, cell lysates were acquired with RIPA buffer, and ADP-ribosylation was performed with 2.5 μg lysate and 300 nM toxin as described above.

Cell viability assay. For determination of cytotoxicity, HEK-293 cells were cultured in complete medium in 96-well plates. Cells were incubated for 48 h with the indicated concentrations of DT and PMT-DTa chimeras at 37°C, and cell viability was determined by measuring the metabolic activity of cells, using the CellTiter-Blue assay (Promega, Mannheim, Germany). Fluorescent products were measured on a multiwell fluorescence reader (Infinite M200; Tecan, Crailsheim, Germany) according to the manufacturer's protocol.

Detection of protein biosynthesis. HEK-293 cells were incubated overnight with PMT-DTa or DT (3 nM) in 6-well plates. After changing from complete medium to medium without FCS, 1 μCi/ml [^{14}C]leucine was added and incubated for 1 h at 37°C. The cells were washed three times with PBS (4°C), and the proteins were precipitated with 10% trichloroacetic acid (TCA) (30 min, 4°C). The solution was centrifuged at 13,000 rpm for 20 min. The pellet was transferred to 500 μl PBS and 2 ml Ultima Gold scintillation solution. The radioactivity of the incorporated [^{14}C]leucine was measured with a liquid scintillation counter (Tri-Carb 2900TR; Packard).

Immunoblot analysis. Proteins were analyzed by immunoblotting after SDS-polyacrylamide gel electrophoresis. Anti-DTa antibody (GTX28308) was purchased from Acris Antibodies (Herford, Germany). Anti-PMT antibody was produced against a peptide in the N-terminal part of the toxin (aa 380 to 400). An enhanced chemiluminescence detection reagent (100 mM Tris-HCl [pH 8.0], 1 mM luminol (Fluka), 0.2 mM p-coumaric acid, and 3 mM H$_2$O$_2$) was used to detect binding of a horseradish peroxidase-coupled secondary antibody with an LAS-3000 imaging system (Fujifilm).

Fluorescence labeling. PMT-DTa and PMT were N-terminally conjugated to fluorescein by using the sortase method (35, 36) and the fluorophore 5(6)-fluorescein-NH-Ahx-LPRT-COOMe (Thermo Scientific, Ulm, Germany).

Recombinant sortase A from *Staphylococcus aureus* (SrtA$_{Staph}$) with an N-terminal hexahistidine tag was expressed in *Escherichia coli* cells and purified according to the method of Ton-That et al. (37). Sortase-mediated labeling of PMT was performed according to the method described by Antos et al. (36), with slight alterations. PMT or PMT-DTa was incubated with 5(6)-fluorescein-NH-Ahx-LPRT-COOMe (500 μM) and SrtA$_{Staph}$ (20 μM) for 1 h at 37°C. SrtA$_{Staph}$ was removed by incubation with Protino Ni-IDA resin (Macherey-Nagel, Dueren, Germany). An excess of the fluorophore was removed by using a PD-10 column (GE Healthcare, Buckinghamshire, United Kingdom). Fluorophore-labeled PMT was separated by SDS-PAGE, and the fluorescence was detected by illuminating the SDS gel with a laser (488 nm) in a Typhoon 9200 scanner (GE Healthcare).

Fluorescence microscopy. Caco-2 cells were grown on HCl-washed glass coverslips to a confluence of 60 to 80%. Cells were intoxicated with labeled PMT or PMT-DTa (0.5 μM) for different times: 30 min for early endosomal antigen 1 (EEA1) staining, 30 min for Rab5, 1 h for Rab7, 1 h for Rab11, 40 min for CTR433, and 1 h for LAMP1. Cells were washed with PBS and fixed with 4% paraformaldehyde in PBS for 15 min at room temperature. Thereafter, cells were washed with PBS and permeabilized with 0.15% Triton X-100 in PBS for 10 min. Cells were blocked for 1 h in a blocking solution (PBS with 1% bovine serum albumin and 0.05% Tween 20). Next, cells were incubated with the primary antibody diluted in the blocking solution for 1 h. After washing with PBS with 0.05% Tween 20, cells were incubated with a 1:200 dilution of Alexa 568-conjugated secondary antibody in blocking solution for 1 h. For Rab7 staining, cells were fixed with methanol and 1 mM EGTA (−20°C) for 15 min. After washing with PBS, the cells were permeabilized and blocked for 1 h with blocking buffer (PBS with 5% normal goat serum [NGS] and 0.3% Triton X-100). The cells were then incubated with the Rab7 antibody in blocking buffer at 4°C overnight. After washing with PBS with 0.05% Tween 20 (PBS-T), the cells were incubated for 1 h with the secondary antibody. Again, cells were washed three times with PBS with 0.05% Tween 20 and once with PBS. Water was removed from the coverslips by subsequent

washes with 70% and 100% ethanol. Cells were mounted with Mowiol 4-88 (Calbiochem, La Jolla, CA) containing 2.5% 1,4-diazabicyclo-[2.2.2]octane. Fixed samples were analyzed with an inverted Axiovert 200 M microscope (Carl Zeiss) with a Yokogawa (Tokyo, Japan) CSU-X1 spinning disc equipped with an emission filter wheel and 488-nm/561-nm laser lines.

Rabbit anti-Rab7 (9367) and rabbit anti-Rab11 (3539) were purchased from Cell Signaling Technology and used at a 1:200 dilution. Rabbit anti-Rab5 (sc-598), mouse anti-LAMP1 (sc-20011), and goat anti-EEA1 (sc-6415) were purchased from Santa Cruz Biotechnology and used at a 1:200 dilution. Mouse anti-CTR433 was used at a 1:100 dilution.

RESULTS

A chimeric protein comprising the ADP-ribosyltransferase domain of DT (DTa) and PMT was constructed according to the scheme presented in Fig. 1. To this end, the DNA of PMT encoding the full-length protein (aa 1 to 1285) was fused to the catalytically active domain of diphtheria toxin (DTa; aa 26 to 216). To avoid concomitant activity of PMT, a catalytically inactive point mutant of the C3 domain of PMT was utilized (C1165S mutant).

Proteins were expressed and purified as glutathione S-transferase (GST) fusion proteins and subsequently released from the GST tag by thrombin cleavage. PMT-DTa fusion proteins were analyzed by SDS-PAGE and immunoblotting (Fig. 1B). Migration of fusion proteins in SDS-PAGE gels stained with Coomassie blue was in agreement with the calculated masses of the proteins. An antibody against the N terminus of PMT recognized PMT-DTa and wild-type PMT (PMT^{wt}) but not DT in the immunoblot analysis. Additionally, a DTa-directed antibody recognized PMT-DTa and DT but not PMT, confirming the complete expression of the chimera with the C-terminally fused DTa fragment.

The activity of the fused ADP-ribosyltransferase domain DTa was initially tested using an *in vitro* assay. PMT-DTa but not PMT^{wt} induced ADP-ribosylation of EF-2 in a concentration-dependent manner (Fig. 2A). A time-dependent intoxication of HEK-293 cells by PMT-DTa was performed. Cell viability was measured by the CellTiter-Blue assay. After 22 h, a cytotoxic effect of PMT-DTa was detectable; the toxic effect increased during the incubation time of 48 h (Fig. 2B). In contrast, native PMT^{wt} affected cell viability only minimally after cell treatment and incubation for 48 h. The minor decrease in cell viability after 48 h may have been due to the mitogenic effect of PMT^{wt}, which leads to faster medium wastage.

Modification of EF-2 *in vivo* by PMT-DTa was tested by a "post-ADP-ribosylation" assay. To this end, HEK-293 cells were intoxicated with PMT-DTa (3 nM) for the indicated times. Thereafter, cells were lysed, and an ADP-ribosylation assay with fresh toxin in the presence of ^{32}P-NAD$^+$ was performed. As shown in Fig. 2C, increasing the time of cell incubation with PMT-DTa led to a reduction of [^{32}P]ADP-ribosylation of EF-2, indicating a modification of EF-2 with unlabeled ADP-ribose during cell intoxication.

The consequence of ADP-ribosylation of EF-2 by DTa is a blockade of protein synthesis (34). Therefore, we determined protein synthesis by measuring the incorporation of [^{14}C]leucine into HEK-293 cells. To do so, we treated cells without and with PMT-DTa, DT, or DTa in the presence of labeled leucine. After 24 h, cells were lysed, and incorporation of [^{14}C]leucine into cellular proteins was determined. As expected, ADP-ribosylation of EF-2 by PMT-DTa or DT impaired protein synthesis, as detected by diminished incorporation of [^{14}C]leucine (Fig. 2D). In contrast,
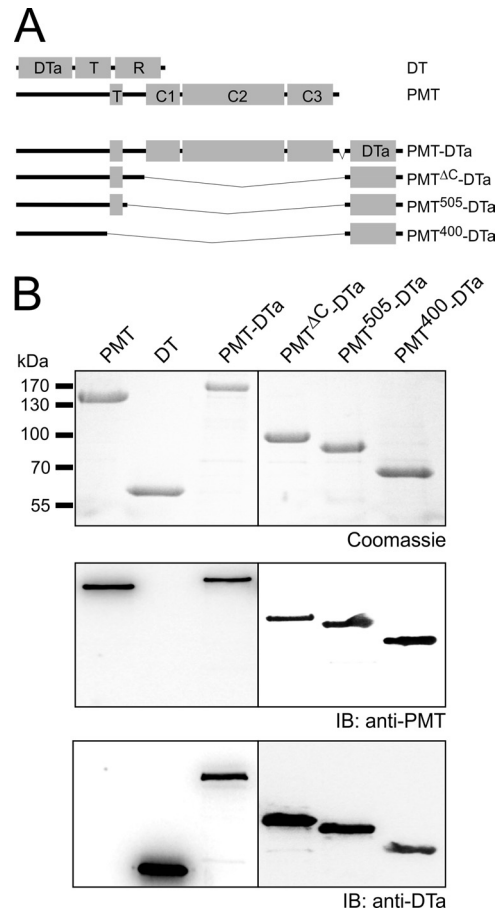

FIG 1 PMT-DTa chimeras. (A) Schematic representation of the PMT-DTa chimeras used in this study. Diphtheria toxin (DT) consists of three domains: the ADP-ribosylation domain (DTa), the translocation domain (T), and the receptor binding domain (R). The 146-kDa toxin PMT consists of several domains. In the scheme, the translocation domain (T; 2 amphipathic helices) and the 3 domains in the C-terminal part (C1 to C3) are indicated. The PMT-DTa chimera comprises full-length PMT (aa 1 to 1285) fused to the active domain of diphtheria toxin (DTa; aa 26 to 216). PMT$^{\Delta C}$-DTa comprises the N terminus of PMT, without the C1, C2, and C3 domains (aa 1 to 582), fused to DTa. PMT^{505}-DTa consists of the N-terminal part of PMT (aa 1 to 505) fused to DTa. PMT^{400}-DTa consists of the N-terminal part of PMT (aa 1 to 400), without the 2 amphipathic helices, fused to DTa. (B) SDS-PAGE and immunoblot analysis (IB) of purified recombinant PMT, PMT-DTa chimeras, and DT. Purified recombinant PMT and PMT-DTa chimeras were analyzed by SDS-PAGE (upper panel) and by immunoblotting with anti-PMT antibody (middle panel) or anti-DTa antibody (lower panel).

DTa, the ADP-ribosylation domain of DT without receptor binding and translocation domains, did not affect protein synthesis, though the ADP-ribosylation activity of DTa was able to modify EF-2 in an *in vitro* approach (see Fig. S1 in the supplemental material).

Intoxication of cells by PMT-DTa was studied by monitoring the morphology of HEK-293 cells. Treatment of HEK-293 cells with PMT-DTa led to a rounding of cells comparable to the effect of DT. As expected, treatment of HEK-293 cells with active PMT^{wt} did not cause rounding but induced a flattened phenotype of cells (Fig. 2E).

Characterization of cell uptake of PMT-DTa. The PMT-DTa chimera consists of the complete PMT toxin, encompassing all
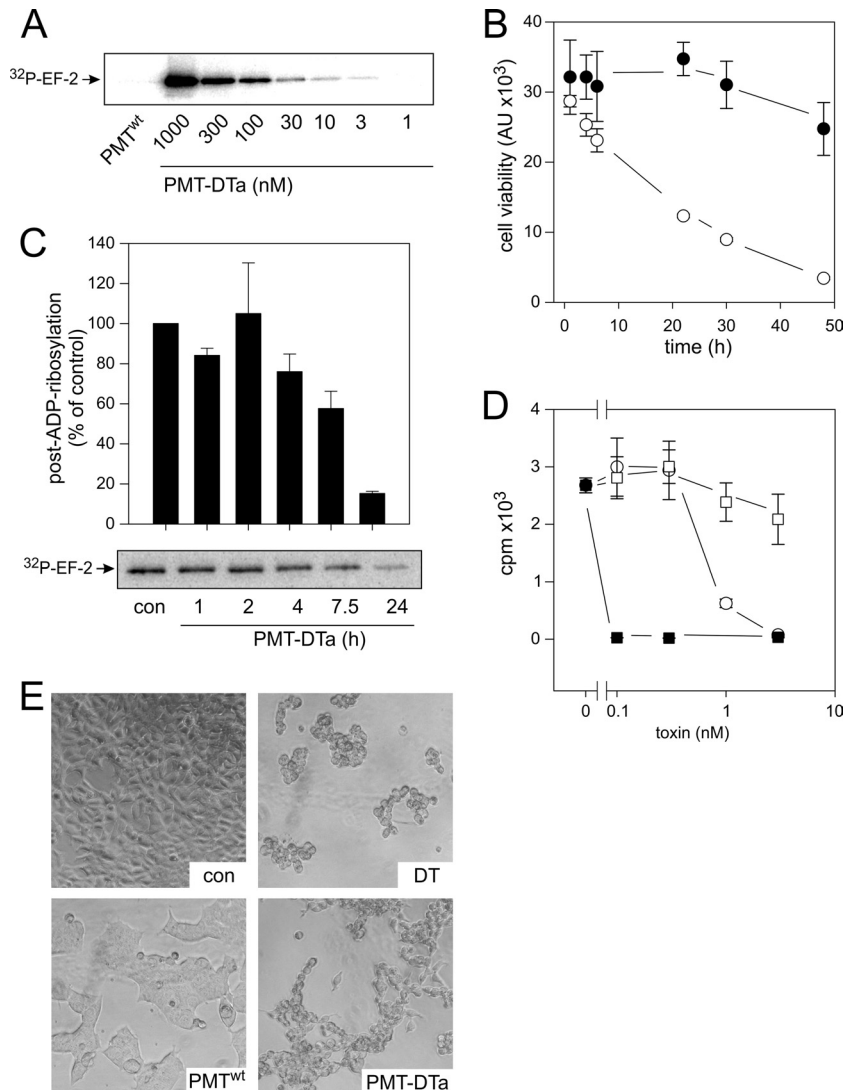
FIG 2 Cytotoxic effects of PMT-DTa chimera. (A) ADP-ribosylation of EF-2 was performed *in vitro* with the indicated concentrations of PMT-DTa and PMT[wt] (1 μM), as described in Materials and Methods. (B) Time-dependent effect of PMT-DTa on cell viability. HEK-293 cells were treated with PMT-DTa (open circles) or PMT[wt] (filled circles) (3 nM for each) for the indicated times, and cell viability was subsequently determined. Data shown are arbitrary units (AU) of fluorescence intensity. (C) Post-ADP-ribosylation of EF-2. HEK-293 cells were incubated with PMT-DTa (3 nM) for the indicated times, and cell lysates were subsequently prepared. Post-ADP-ribosylation assays were performed with ^{32}P-NAD$^+$ as described in Materials and Methods. Data shown are quantifications of ADP-ribosylation calculated by using Image Quant (GE Healthcare). The strongest signal produced by [^{32}P]ADP-ribosylation was defined as 100%. con, control. (D) PMT-DTa inhibits protein synthesis. HEK-293 cells were treated with or without PMT-DTa (open circles), DT (filled squares), or DTa (open squares) at the indicated concentrations overnight. Thereafter, incorporation of [^{14}C]leucine into newly synthesized proteins was determined. (E) Morphological changes of intoxicated cells. HEK-293 cells were grown to near confluence and treated with DT, PMT[wt], or PMT-DTa (3 nM for each). After 48 h, phase-contrast micrographs were taken. Data shown are representative results for at least three independent experiments. Quantified measurements are given as means ± standard errors (SE) ($n = 3$).

domains, which are important for receptor binding, uptake into endocytic vesicles, and translocation to the cytosol, whereas the DTa fragment consists only of the catalytically active fragment, without any receptor binding or translocation domain. To exclude any unspecific uptake of the PMT-DTa chimera by the DTa fragment, we performed competition experiments with PMT-DTa and the inactive PMT[C1165S] mutant. To this end, intoxication of HEK-293 cells was determined by measuring the PMT-DTa-induced ADP-ribosylation of EF-2. Treatment of HEK-293 cells with PMT-DTa (3 nM) resulted in a strong reduction of [^{32}P]ADP-ribosylation in the post-ADP-ribosyla-

tion assay (Fig. 3A). Addition of increasing concentrations of PMT[C1165S] to PMT-DTa-intoxicated cells rescued the cells from EF-2 ADP-ribosylation, as demonstrated by increasing signals in the post-ADP-ribosylation assay. A ratio of PMT-DTa to PMT[C1165S] of 1 to 100 or 1 to 300 effectively reduced intoxication by PMT-DTa.

To further analyze the uptake of the PMT-DTa chimera, we tested whether the translocation of PMT-DTa from endocytic vesicles into the cytosol depended on a low pH of endosomes. HEK-293 cells were preincubated with bafilomycin A1, an inhibitor of vacuolar H$^+$-ATPases, to prevent acidification of endosomes. The
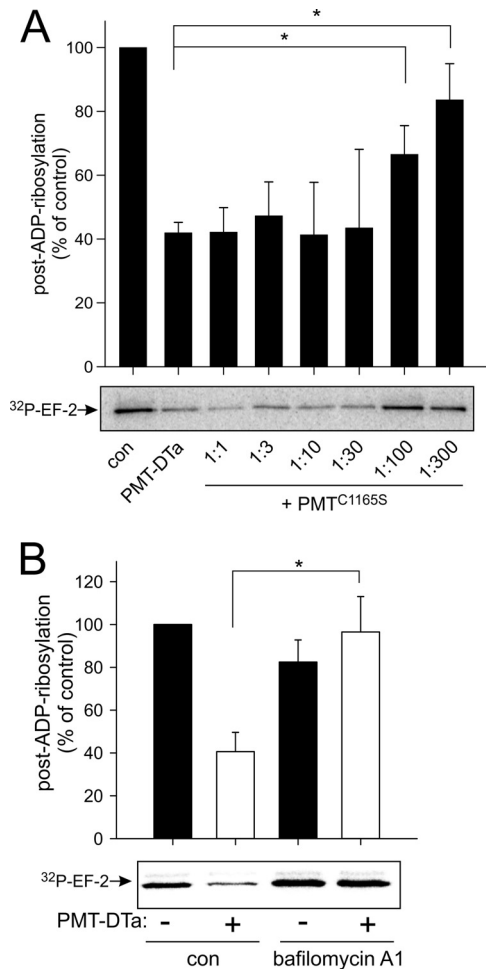
FIG 3 Cellular uptake of PMT-DTa chimera. (A) Competition in cell uptake. HEK-293 cells were treated with 0.3 nM PMT-DTa and increasing concentrations of PMT^{C1165S} (as indicated). After 6 h, the medium was replaced with toxin-free medium and the incubation continued overnight. Cells were lysed, and post-ADP-ribosylation assays with ^{32}P-NAD$^+$ were performed as described in Materials and Methods. (B) Influence of inhibition of endosome acidification by bafilomycin A1 on uptake of PMT-DTa. HEK-293 cells were treated without or with bafilomycin A1 (30 nM) for 30 min. Cells were intoxicated with PMT-DTa (3 nM) for 6 h, and the medium was replaced with fresh medium. After overnight incubation, cells were lysed, and post-ADP-ribosylation assays with ^{32}P-NAD$^+$ were performed. Data shown are quantifications of ADP-ribosylation calculated by using Image Quant (GE Healthcare). The strongest signal produced by [^{32}P]ADP-ribosylation was defined as 100%. Data are representative results from at least three independent experiments. Quantified measurements are given as means ± SE ($n = 3$). Statistical significance was assessed by paired Student's t test. *, $P < 0.05$.

cells were then treated with PMT-DTa, and ADP-ribosylation of EF-2 was determined, utilizing the post-ADP-ribosylation assay. As shown in Fig. 3B, bafilomycin A1 blocked PMT-DTa-induced ADP-ribosylation of EF-2 and rescued the [^{32}P]ADP-ribosylation signal. Thus, the uptake of PMT-DTa depends on a low pH of endosomes.

Furthermore, uptake into endocytic compartments and intracellular trafficking of PMT-DTa were studied by spinning disc microscopy with fluorescently labeled toxin. Therefore, PMT-DTa and PMT were N-terminally transacylated by the enzyme sortase from *Staphylococcus aureus* (SrtA$_{Staph}$), using a synthetic peptide coupled to a fluorophore. Sortase-mediated transacylation depends on the recognition motif (LPRT) in the peptide and on glycine residues in the N terminus of the second protein, which were present in both constructs, PMT-DTa and PMT, due to the thrombin cleavage site. Hence, PMT-DTa and PMT were labeled with fluorescein at the N terminus and purified from sortase and residual fluorophore as shown in Fig. 4A. Colocalization studies were performed in Caco-2 cells because their morphology is advantageous for confocal microscopy. In contrast to HEK-293 cells, Caco-2 cells display a large portion of cytosol and increased cell height, favoring better representation of vesicles. Caco-2 cells were treated with fluorescein-labeled PMT-DTa or PMT for different times. Thereafter, cells were fixed and cellular compartments were visualized by specific marker proteins, using immunofluorescence. Rab5 and EEA1 were used as markers of early endosomes. Rab7 was used as a marker of late endosomes. Rab11 was used as a marker of recycling endosomes, LAMP-1 as a lysosomal marker, and CTR433 as a Golgi marker. As shown in Fig. 4B, PMT-DTa colocalized with EEA1, a marker of early endosomes. Colocalization with a marker of late endosomes (Rab7) was detectable with an intoxication time of 60 min. To prove that the intracellular trafficking of PMT was not hampered by the fusion to DTa, we additionally studied the trafficking of PMT. PMT also colocalized with markers of early endosomes (EEA1 and Rab5) and late endosomes (Rab7) (Fig. 4C). Colocalization of PMT and PMT-DTa was calculated by an overlay approach (see Fig. S2 in the supplemental material). Moreover, we did not detect any colocalization of PMT with markers of other compartments, such as recycling endosomes, lysosomes, or the Golgi apparatus.

Further chimeras of PMT-DTa were created to characterize the minimal region of PMT to serve as a transporter of the fused DTa domain. Three fusions of DTa and PMT were generated by standard PCR techniques. One construct lacks the C1 to C3 domains (PMT$^{\Delta C}$-DTa), and one is missing the complete sequence downstream of the translocation domain of PMT (PMT^{505}-DTa). PMT^{400}-DTa consists only of the N-terminal part of PMT, without the putative translocation domain.

The activity of the fused ADP-ribosyltransferase domain (DTa) was tested using an *in vitro* assay. Cell lysates were incubated with chimeras or activated DT and ^{32}P-NAD$^+$-containing ADP-ribosylation buffer. All chimeras and activated DT (38, 39) exhibited catalytic activity as measured by ADP-ribosylation of EF-2. Whereas all tested chimeras were active, the extents of ADP-ribosylation varied (Fig. 5A). The rank order of the degree of EF-2 modification by PMT-DTa chimeras was as follows: PMT^{505}-DTa ≥ PMT^{400}-DTa = PMT$^{\Delta C}$-DTa > PMT-DTa. Moreover, we trypsin activated PMT-DTa fusions as was done for DT. Trypsin activation increased the activity of DT ~15-fold. However, the activity of PMT-DTa fusions was affected only 2-fold by trypsin treatment (Fig. 5B).

Next, we tested the cell toxicity of DT and PMT-DTa chimeras. HEK-293 cells were intoxicated with fusion constructs (concentration range of 300 pM to 30 nM), and cell viability after 48 h was determined by the CellTiter-Blue assay (Fig. 5C). Determination of cell toxicity revealed the strongest effect for full-length PMT-DTa, followed by PMT^{505}-DTa and PMT$^{\Delta C}$-DTa, which showed nearly equal potencies. PMT^{400}-DTa had no impact on cell viability at the tested concentrations.
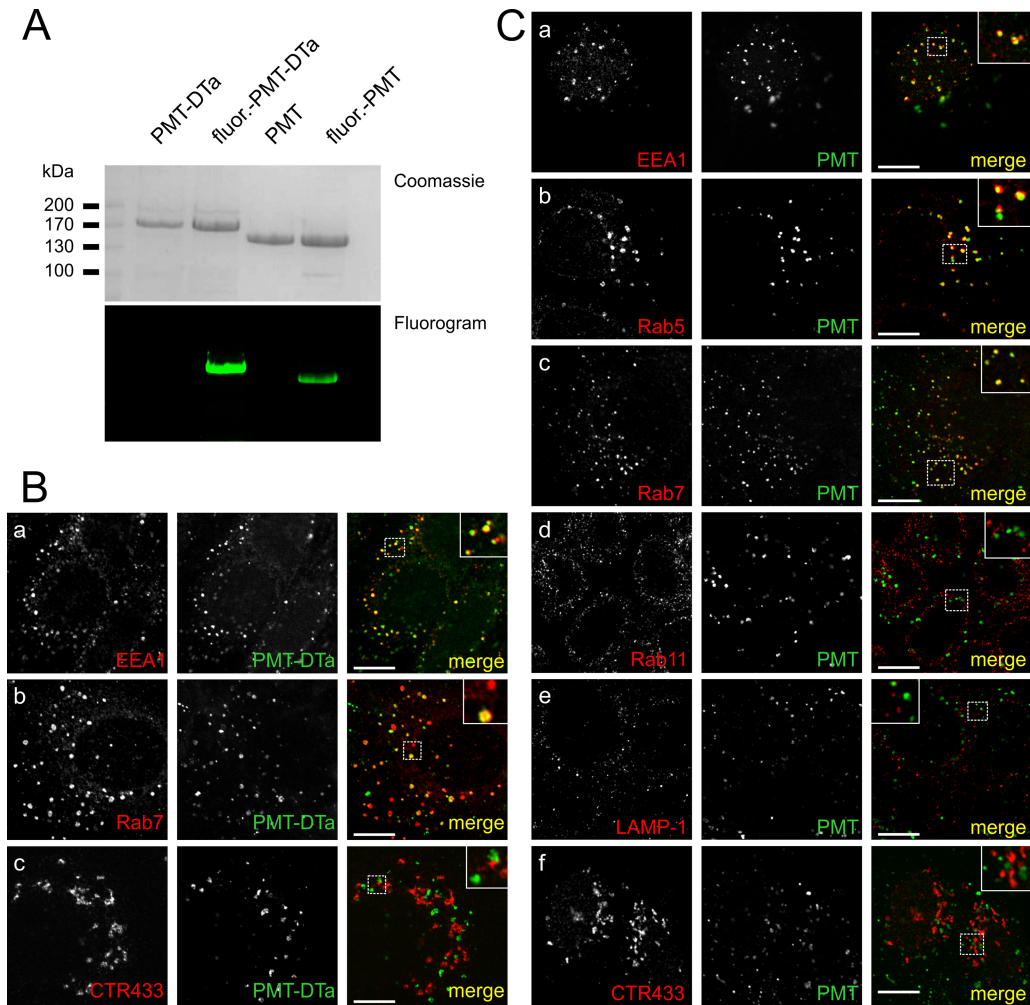
FIG 4 Colocalization of PMT-DTa and PMT with early and late endosome markers. (A) N-terminal labeling of PMT-DTa and PMT with fluorescein fluorophore by use of SrtA$_{Staph}$. A Coomassie-stained gel and a fluorogram (488 nm) of untreated or fluorescence-labeled PMT-DTa and PMT are shown. (B and C) Colocalization of PMT-DTa and PMT with endosome markers. Toxin-treated (0.5 μM) cells were fixed, stained with the indicated antibodies, and analyzed by fluorescence microscopy. Cellular compartments were identified by specific antibodies and an Alexa 568-conjugated secondary antibody (left panels). Fluorescein-labeled toxin is shown in the middle panels. Colocalization is depicted in yellow (right panels). Insets show a magnification of the regions marked with dotted lines. Bars, 10 μm. (B) Intracellular trafficking of labeled PMT-DTa. Colocalization of PMT-DTa was detectable with markers of early endosomes and late endosomes. No colocalization was detectable with a marker of the Golgi apparatus. (a) Early endosome (EEA1); (b) late endosome (Rab7); (c) Golgi apparatus (CTR433). (C) Intracellular trafficking of labeled PMT^{wt}. Colocalization of PMT was detectable with markers of early endosomes and late endosomes. No colocalization was detectable with markers of lysosomes, recycling endosomes, or the Golgi apparatus. (a) Early endosome (EEA1); (b) early endosome (Rab5); (c) late endosome (Rab7); (d) recycling endosome (Rab11); (e) lysosome (LAMP-1); (f) Golgi apparatus (CTR433).

DISCUSSION

Bacterial protein toxins, i.e., exotoxins, are multifunctional proteins composed of various domains with distinct tasks. To target intracellular components of eukaryotic cells, at least two domains are necessary: one domain (B) to induce cellular uptake and one domain (A) which harbors the biological activity (40). In most cases, the uptake domain can be subdivided into a receptor binding (R) domain and a translocation (T) domain. In a large array of toxins, the receptor binding domain induces binding and endocytosis into vesicular compartments, and the translocation domain allows the transport of the A domain from inside the vesicle into the cytosol. Studies from recent years have shown that it is possible to utilize the receptor binding/translocation domain of exotoxins to transport a cargo protein into eukaryotic cells (41–45). Here we analyzed the transport of a non-cell-permeating toxin fragment (DTa) by using PMT as a transporter. We demonstrate that the DTa domain itself does not impair protein synthesis of cells (Fig. 2D), although ADP-ribosylation activity remains *in vitro* (see Fig. S1 in the supplemental material). This indicates that DTa is insufficient to induce its own cellular uptake. Therefore, we constructed various chimeric proteins of PMT and the active domain of diphtheria toxin (DTa), starting with a full-length construct of PMT fused C-terminally to DTa (PMT-DTa). To avoid concurrent biological activities of the fusion of full-length PMT and DTa, a catalytically inactive point mutant of PMT (C1165S mutant) (26, 46) was used for PMT-DTa. Functionality of the PMT-fused DTa domain was confirmed by determination of the ADP-ribosyltransferase activity toward EF-2. PMT-DTa was able to modify EF-2 in an *in vitro* ADP-ribosylation assay, whereas PMT^{wt} had no effect on EF-2.
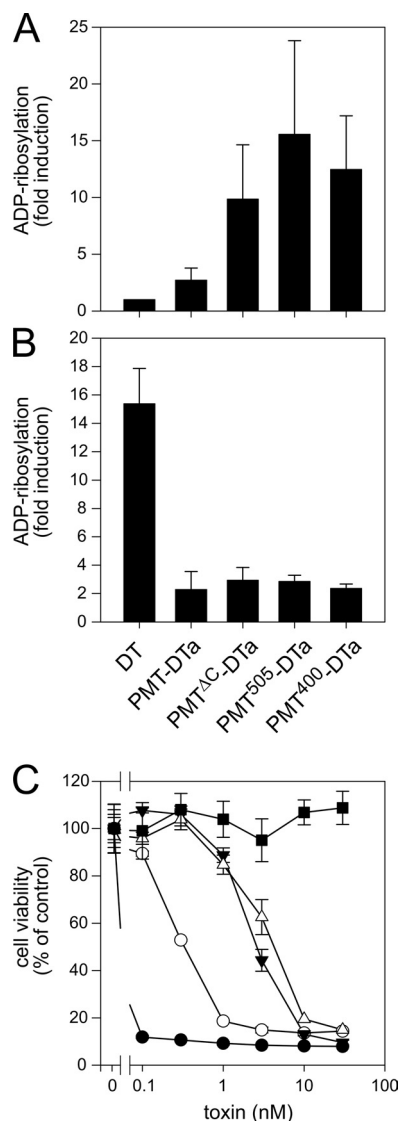
FIG 5 Minimal region of PMT to induce cellular uptake. (A) ADP-ribosylation activities of DT and PMT-DTa fusions. HEK-293 cell lysates were incubated with toxin (300 nM for each), and ADP-ribosylation of EF-2 (^{32}P-EF-2) was measured as described in Materials and Methods. The quantification of ADP-ribosylation was performed by using Image Quant (GE Healthcare), and data are shown as the fold induction over the level with DT. (B) DT and PMT-DTa chimeras were treated with trypsin as described in Materials and Methods. ADP-ribosylation of EF-2 was performed as described before. ADP-ribosylation of EF-2 by trypsin-treated toxin was calculated as the fold induction over the level with untreated toxin. Data shown are representative results from at least three independent experiments and are given as means and SE ($n = 3$). (C) Cell viability is compromised in a concentration-dependent manner by PMT-DTa fusions. HEK-293 cells were intoxicated with DT or PMT-DTa chimeras at the indicated concentrations (black circles, DT; open circles, PMT-DTa; black triangles, PMT^{505}-DTa; open triangles, PMT$^{\Delta C}$-DTa; and black squares, PMT^{400}-DTa). Subsequently, cell viability was determined by the CellTiter-Blue assay. Data shown are cell viabilities normalized to the control and are given as means ± SE ($n = 3$).

Time-dependent intoxication of HEK-293 cells was tested with PMT-DTa and showed a strong reduction of metabolic activity. In contrast, PMT^{wt} did not impair cell viability. These data correlated with intracellular PMT-DTa-induced ADP-ribosylation, which

was evident in a post-ADP-ribosylation assay. To further characterize the uptake of the PMT-DTa chimera, specific steps of cell intoxication were studied. Competition studies of PMT-DTa with PMT^{C1165S} revealed binding of PMT-DTa and PMT to identical receptors. Translocation of PMT-DTa into the cytosol depends on acidification of the endosome, as revealed by inhibition of EF-2 ADP-ribosylation by PMT-DTa upon treatment with an inhibitor of vacuolar H$^+$-ATPase (47). This is in congruence to previous findings that the biological effect of PMT depends on acidification during uptake (11, 21). To follow intracellular trafficking, PMT-DTa was labeled site specifically at the N terminus with a fluorescent epitope. To this end, a recently described method utilizing the enzyme sortase from *Staphylococcus aureus* was employed (35, 36). The key advantage of the method is the small size of the label and the specificity of the labeled site. Hence, the possibility of impairing the trafficking route by the fluorescence label is reduced to a great extent. Colocalization studies identified labeled PMT-DTa in early and late endosomes. It is known that the pH of endosomes is acidified during trafficking from early to late endosomes (48). Therefore, the data suggest that PMT-DTa translocates from these compartments into the cytosol. In addition, similarly labeled PMT^{wt} was found to colocalize with markers of early and late endosomes, indicating that the PMT-DTa chimera behaves like PMT^{wt}. In contrast, PMT was not found in other compartments, such as recycling endosomes, lysosomes, or the Golgi apparatus. Thus, our results confirm previous findings that PMT traffics through early and late endosomes (49).

To determine the minimal region of PMT sufficient for cellular uptake of DTa, truncations of PMT were constructed. The various chimeric fusion proteins exhibited different efficiencies in ADP-ribosylation of EF-2. While the short PMT-DTa chimeras (PMT$^{\Delta C}$-DTa, PMT^{505}-DTa, and PMT^{400}-DTa) exhibited strong ADP-ribosylation activity toward EF-2, comparable to that of activated DT, the fusion protein PMT-DTa was surprisingly less active. Differences in the activity of the DTa domain might be due to structural restrictions of the fusion protein. Wild-type DT exhibits full ADP-ribosyltransferase activity only after proteolytic cleavage and reduction of the remaining disulfide bond, i.e., the biologically active DTa fragment has to be set free from the full-length toxin (38, 39). Accordingly, trypsin treatment of PMT-DTa fusions increased ADP-ribosylation activity. However, the increase of ADP-ribosylation activity of the PMT-DTa fusion was only 2-fold, compared to an ~15-fold increase detected with DT. These results indicate that in contrast to the case with DT, the ADP-ribosyltransferase activity was hardly inhibited by the overall structure of the fusion proteins. However, we cannot exclude that a specific proteolytic step is involved in the translocation and/or action of PMT. In this respect, it is interesting that CNF1, which exhibits sequence similarity with PMT over a large N-terminal region, is apparently proteolytically processed during its cellular uptake (50). Whether this is also true for PMT remains to be analyzed. In the next step, we analyzed the ability of the PMT-DTa fusions to intoxicate eukaryotic cells by determination of the metabolic activity of HEK-293 cells. The fusion protein, comprising full-length PMT fused to DTa (PMT-DTa), was the most active construct. Whereas PMT^{400}-DTa did not intoxicate cells, the other constructs (PMT^{505}-DTa and PMT$^{\Delta C}$-DTa) exhibited up to 10 times less activity than that of PMT-DTa. This is a surprising finding, because constructs that were highly active in ADP-ribosylation *in vitro* were found to be less potent in cell intoxication.

This finding allows important conclusions to be drawn about the efficiency of the transport of fusion toxins and highlights the relevance of a coordinated function of the full-length multidomain toxin.

Our data indicate that a region of PMT as small as the N-terminal region covering residues 1 to 505 is suitable to induce uptake of a C-terminally fused protein such as DTa. This is in agreement with the proposed domain structure of PMT, including a receptor binding site in the far N terminus followed by a translocation domain (21). This model is strengthened by the finding that a shortened PMT fragment (PMT^{400}-DTa) without the full translocation domain was not able to transport the cargo into the cytosol. PMT$^{\Delta C}$-DTa, which encompasses the N-terminal region of PMT from aa 1 to 582, exhibited the same potency in cell intoxication as PMT^{505}-DTa. The full-length PMT protein is probably optimized in its translocation ability, suggesting that the additional C1 to C3 domains favor a toxin structure which is most rapidly translocated.

In conclusion, we present data showing that PMT can be utilized as a transporter to carry a non-cell-permeating protein (DTa) as a fusion protein into the cytosol of host cells. For this transport, the N terminus of PMT, encompassing residues 1 to 505, most likely covering the receptor binding and translocation domains, is sufficient. Our findings are of major importance for further analysis of the binding and translocation of PMT. For example, the PMT-DTa chimeras can be employed in gene trapping screens as a tool to identify the still unknown receptor of PMT. This screening is much easier with toxins which exhibit strong cytotoxic effects than with toxins which may cause morphological changes but do not kill cells rapidly, such as PMT.

ACKNOWLEDGMENTS

REFERENCES

1. **Harper M, Boyce JD, Adler B.** 2006. *Pasteurella multocida* pathogenesis: 125 years after Pasteur. FEMS Microbiol. Lett. **265:**1–10.
2. **Griego RD, Rosen T, Orengo IF, Wolf JE.** 1995. Dog, cat, and human bites: a review. J. Am. Acad. Dermatol. **33:**1019–1029. doi:10.1016/0190-9622(95)90296-1.
3. **Wilkie IW, Harper M, Boyce JD, Adler B.** 2012. Pasteurella multocida: diseases and pathogenesis. Curr. Top. Microbiol. Immunol. **361:**1–22. doi:10.1007/82_2012_216.
4. **Frandsen PL, Foged NT, Petersen SK, Bording A.** 1991. Characterization of toxin from different strains of *Pasteurella multocida* serotype A and D. Zentralbl. Veterinarmed. B. **38:**345–352.
5. **Horiguchi Y.** 2012. Swine atrophic rhinitis caused by Pasteurella multocida toxin and Bordetella dermonecrotic toxin. Curr. Top. Microbiol. Immunol. **361:**113–129. doi:10.1007/82_2012_206.
6. **Boyce JD, Seemann T, Adler B, Harper M.** 2012. Pathogenomics of Pasteurella multocida. Curr. Top. Microbiol. Immunol. **361:**23–38. doi:10.1007/82_2012_203.
7. **Orth JH, Aktories K.** 2012. Molecular biology of Pasteurella multocida toxin. Curr. Top. Microbiol. Immunol. **361:**73–92. doi:10.1007/82_2012_201.
8. **Orth JH, Fester I, Siegert P, Weise M, Lanner U, Kamitani S, Tachibana T, Wilson BA, Schlosser A, Horiguchi Y, Aktories K.** 2013. Substrate specificity of Pasteurella multocida toxin for alpha subunits of heterotrimeric G proteins. FASEB J. **27:**832–842.
9. **Orth JH, Preuss I, Fester I, Schlosser A, Wilson BA, Aktories K.** 2009.

10. **Tesmer JJ, Berman DM, Gilman AG, Sprang SR.** 1997. Structure of RGS4 bound to AlF4-activated G(i alpha1): stabilization of the transition state for GTP hydrolysis. Cell **89:**251–261.
11. **Rozengurt E, Higgins T, Chanter N, Lax AJ, Staddon JM.** 1990. *Pasteurella multocida* toxin: potent mitogen for cultured fibroblasts. Proc. Natl. Acad. Sci. U. S. A. **87:**123–127.
12. **Wilson BA, Zhu X, Ho M, Lu L.** 1997. *Pasteurella multocida* toxin activates the inositol triphosphate signaling pathway in Xenopus oocytes via G$_{q\alpha}$-coupled phospholipase C-β1. J. Biol. Chem. **272:**1268–1275.
13. **Zywietz A, Gohla A, Schmelz M, Schultz G, Offermanns S.** 2001. Pleiotropic effects of Pasteurella multocida toxin are mediated by Gq-dependent and -independent mechanisms. Involvement of Gq but not G11. J. Biol. Chem. **276:**3840–3845.
14. **Orth JH, Lang S, Taniguchi M, Aktories K.** 2005. Pasteurella multocida toxin-induced activation of RhoA is mediated via two families of G{alpha} proteins, G{alpha}q and G{alpha}12/13. J. Biol. Chem. **280:**36701–36707.
15. **Orth JH, Fester I, Preuss I, Agnoletto L, Wilson BA, Aktories K.** 2008. Activation of Galphai and subsequent uncoupling of receptor-Galphai signaling by Pasteurella multocida toxin. J. Biol. Chem. **283:**23288–23294.
16. **Preuss I, Kurig B, Nürnberg B, Orth JH, Aktories K.** 2009. Pasteurella multocida toxin activates Gbetagamma dimers of heterotrimeric G proteins. Cell. Signal. **21:**551–558.
17. **Lax AJ, Grigoriadis AE.** 2001. *Pasteurella multocida* toxin: the mitogenic toxin that stimulates signalling cascades to regulate growth and differentiation. Int. J. Med. Microbiol. **291:**261–268.
18. **Preuss I, Hildebrand D, Orth JH, Aktories K, Kubatzky KF.** 2010. Pasteurella multocida toxin is a potent activator of anti-apoptotic signalling pathways. Cell. Microbiol. **12:**1174–1185.
19. **Aminova LR, Wilson BA.** 2007. Calcineurin-independent inhibition of 3T3-L1 adipogenesis by *Pasteurella multocida* toxin: suppression of Notch1, stabilization of beta-catenin and pre-adipocyte factor 1. Cell. Microbiol. **9:**2485–2496.
20. **Rasmussen SG, DeVree BT, Zou Y, Kruse AC, Chung KY, Kobilka TS, Thian FS, Chae PS, Pardon E, Calinski D, Mathiesen JM, Shah ST, Lyons JA, Caffrey M, Gellman SH, Steyaert J, Skiniotis G, Weis WI, Sunahara RK, Kobilka BK.** 2011. Crystal structure of the beta2 adrenergic receptor-Gs protein complex. Nature **477:**549–555.
21. **Baldwin MR, Lakey JH, Lax AJ.** 2004. Identification and characterization of the Pasteurella multocida toxin translocation domain. Mol. Microbiol. **54:**239–250.
22. **Brothers MC, Ho M, Maharjan R, Clemons NC, Bannai Y, Waites MA, Faulkner MJ, Kuhlenschmidt TB, Kuhlenschmidt MS, Blanke SR, Rienstra CM, Wilson BA.** 2011. Membrane interaction of Pasteurella multocida toxin involves sphingomyelin. FEBS J. **278:**4633–4648.
23. **Kitadokoro K, Kamitani S, Miyazawa M, Hanajima-Ozawa M, Fukui A, Miyake M, Horiguchi Y.** 2007. Crystal structures reveal a thiol protease-like catalytic triad in the C-terminal region of Pasteurella multocida toxin. Proc. Natl. Acad. Sci. U. S. A. **104:**5139–5144.
24. **Kamitani S, Kitadokoro K, Miyazawa M, Toshima H, Fukui A, Abe H, Miyake M, Horiguchi Y.** 2010. Characterization of the membrane-targeting C1 domain in Pasteurella multocida toxin. J. Biol. Chem. **285:**25467–25475.
25. **Geissler B, Tungekar R, Satchell KJ.** 2010. Identification of a conserved membrane localization domain within numerous large bacterial protein toxins. Proc. Natl. Acad. Sci. U. S. A. **107:**5581–5586.
26. **Busch C, Orth J, Djouder N, Aktories K.** 2001. Biological activity of a C-terminal fragment of *Pasteurella multocida* toxin. Infect. Immun. **69:**3628–3634.
27. **Orth JH, Blöcker D, Aktories K.** 2003. His1205 and His1223 are essential for the activity of the mitogenic *Pasteurella multocida* toxin. Biochemistry **42:**4971–4977.
28. **Pullinger GD, Lax AJ.** 2007. Histidine residues at the active site of the Pasteurella multocida toxin. Open Biochem. J. **1:**7–11.
29. **Collier RJ.** 1975. Diphtheria toxin: mode of action and structure. Bacteriol. Rev. **39:**54–85.
30. **Choe S, Bennett MJ, Fujii G, Curmi PMG, Kantardjieff KA, Collier RJ, Eisenberg D.** 1992. The crystal structure of diphtheria toxin. Nature **357:**216–222.
31. **Collier RJ, Cole HA.** 1969. Diphtheria toxin subunit active in vitro. Science **164:**1179–1181.
32. **Honjo T, Nishizuka Y, Hayaishi O.** 1968. Diphtheria toxin-dependent

adenosine diphosphate ribosylation of aminoacryl transferase II and inhibition of protein synthesis. J. Biol. Chem. **243**:3553–3555.

33. **Gill DM, Pappenheimer JAM, Brown R, Kurnick JT.** 1969. Studies on the mode of action of diphtheria toxin. VII. Toxin-stimulated hydrolysis of nicotinamide adenine dinucleotide in mammalian cell extracts. J. Exp. Med. **129**:1–21.

34. **Deng Q, Barbieri JT.** 2008. Molecular mechanisms of the cytotoxicity of ADP-ribosylating toxins. Annu. Rev. Microbiol. **62**:271–288.

35. **Popp MW, Antos JM, Grotenbreg GM, Spooner E, Ploegh HL.** 2007. Sortagging: a versatile method for protein labeling. Nat. Chem. Biol. **3**:707–708.

36. **Antos JM, Chew GL, Guimaraes CP, Yoder NC, Grotenbreg GM, Popp MW, Ploegh HL.** 2009. Site-specific N- and C-terminal labeling of a single polypeptide using sortases of different specificity. J. Am. Chem. Soc. **131**:10800–10801. doi:10.1021/ja902681k.

37. **Ton-That H, Liu G, Mazmanian SK, Faull KF, Schneewind O.** 1999. Purification and characterization of sortase, the transpeptidase that cleaves surface proteins of Staphylococcus aureus at the LPXTG motif. Proc. Natl. Acad. Sci. U. S. A. **96**:12424–12429.

38. **Collier RJ, Kandel J.** 1971. Structure and activity of diphtheria toxin. I. Thiol-dependent dissociation of a fraction of toxin into enzymatically active and inactive fragments. J. Biol. Chem. **246**:1496–1503.

39. **Drazin R, Kandel J, Collier RJ.** 1971. Structure and activity of diphtheria toxin. II. Attack by trypsin at a specific site within the intact toxin molecule. J. Biol. Chem. **246**:1504–1510.

40. **Falnes PO, Sandvig K.** 2000. Penetration of protein toxins into cells. Curr. Opin. Cell Biol. **12**:407–413.

41. **Madshus IH.** 1995. Diphtheria toxin can be used as a vehicle for bringing other proteins into cells. Restor. Neurol. Neurosci. **8**:13–14.

42. **Boquet P, Popoff MR, Giry M, Lemichez E, Bergez-Aullo P.** 1995.

43. **Blanke SR, Milne JC, Benson EL, Collier RJ.** 1996. Fused polycationic peptide mediates delivery of diphtheria toxin A chain to the cytosol in the presence of anthrax protective antigen. Proc. Natl. Acad. Sci. U. S. A. **93**:8437–8442.

44. **Fahrer J, Funk J, Lillich M, Barth H.** 2011. Internalization of biotinylated compounds into cancer cells is promoted by a molecular Trojan horse based upon core streptavidin and clostridial C2 toxin. Naunyn Schmiedebergs Arch. Pharmacol. **383**:263–273. doi:10.1007/s00210-010-0585-7.

45. **Barth H, Blöcker D, Aktories K.** 2002. The uptake machinery of clostridial actin ADP-ribosylating toxins—a cell delivery system for fusion proteins and polypeptide drugs. Naunyn Schmiedebergs Arch. Pharmacol. **366**:501–512.

46. **Ward PN, Miles AJ, Sumner IG, Thomas LH, Lax AJ.** 1998. Activity of the mitogenic *Pasteurella multocida* toxin requires an essential C-terminal residue. Infect. Immun. **66**:5636–5642.

47. **Yoshimori T, Yamamoto A, Moriyama Y, Futai M, Tashiro Y.** 1991. Bafilomycin A1, a specific inhibitor of vacuolar-type H(+)-ATPase, inhibits acidification and protein degradation in lysosomes of cultured cells. J. Biol. Chem. **266**:17707–17712.

48. **Marshansky V, Futai M.** 2008. The V-type H+-ATPase in vesicular trafficking: targeting, regulation and function. Curr. Opin. Cell Biol. **20**:415–426.

49. **Repella TL, Ho M, Chong TPM, Bannai Y, Wilson BA.** 2011. Arf6-dependent intracellular trafficking of Pasteurella multocida toxin and pH-dependent translocation from late endosomes. Toxins **3**:218–241.

50. **Knust Z, Blumenthal B, Aktories K, Schmidt G.** 2009. Cleavage of *Escherichia coli* cytotoxic necrotizing factor 1 is required for full biologic activity. Infect. Immun. **77**:1835–1841.

Inhibition of p21 Rho in intact cells by C3 diphtheria toxin chimera proteins. Methods Enzymol. **256**:297–306.